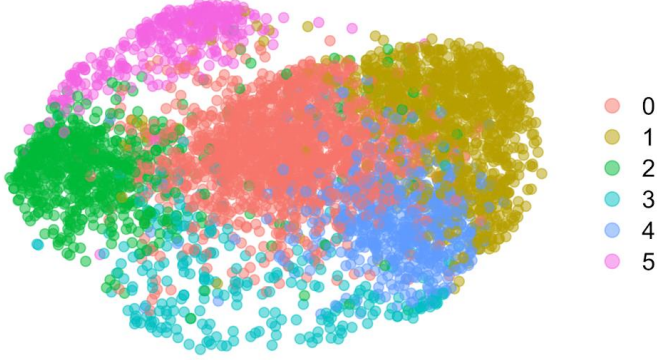
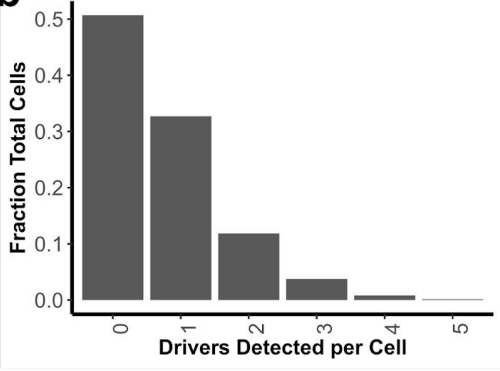
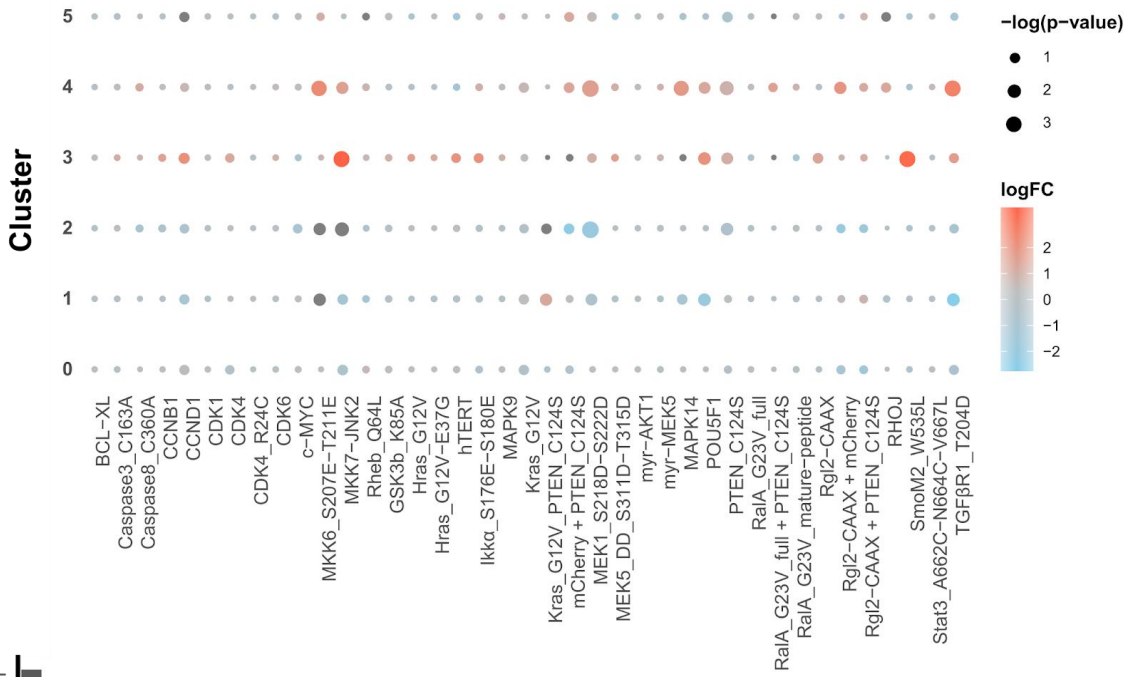
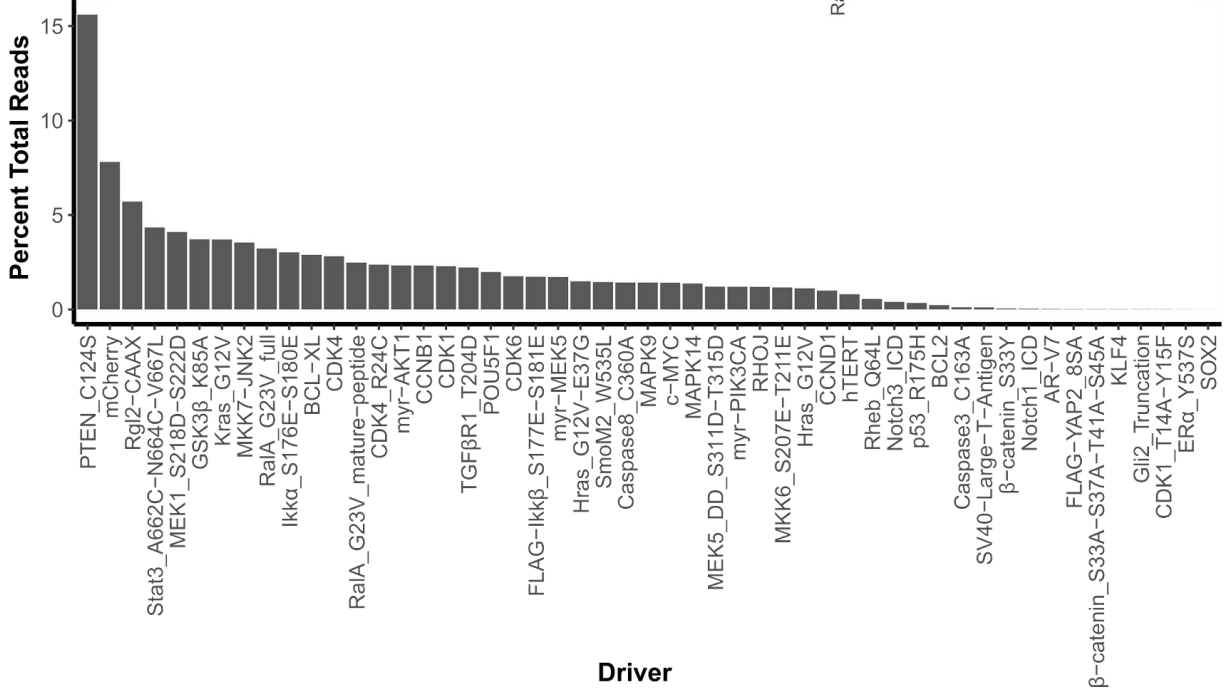


iScience, Volume 24

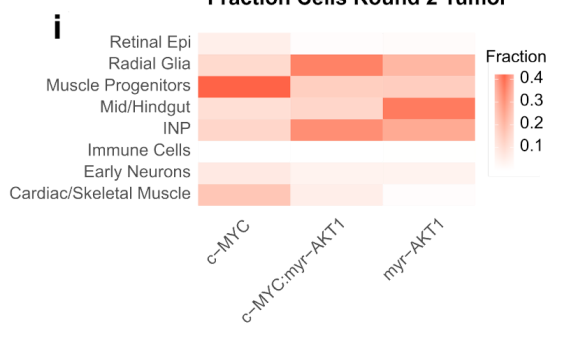
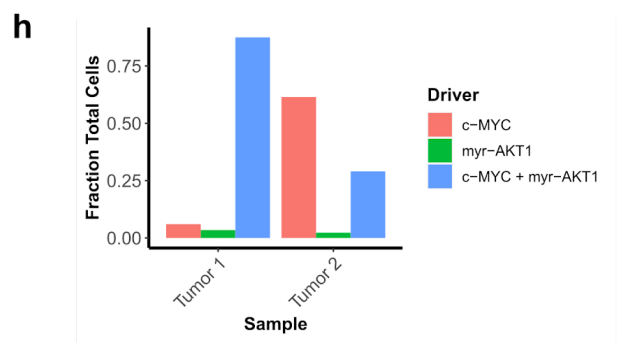
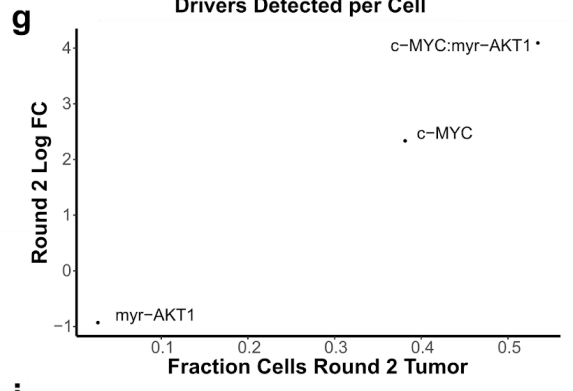
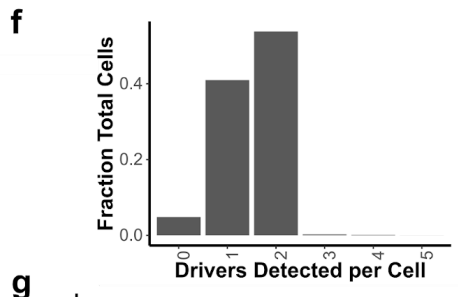
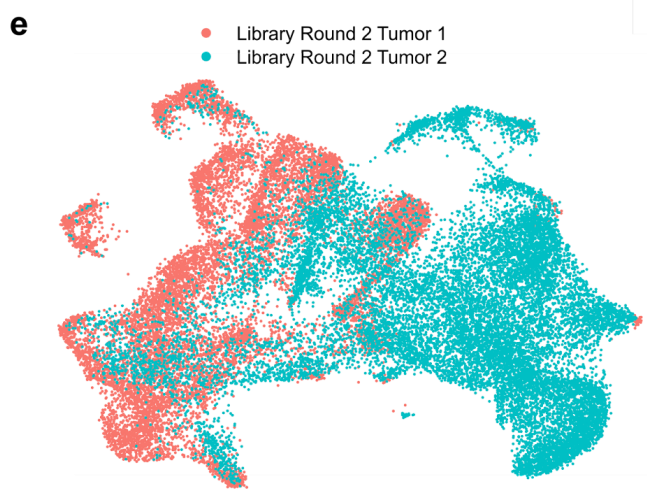
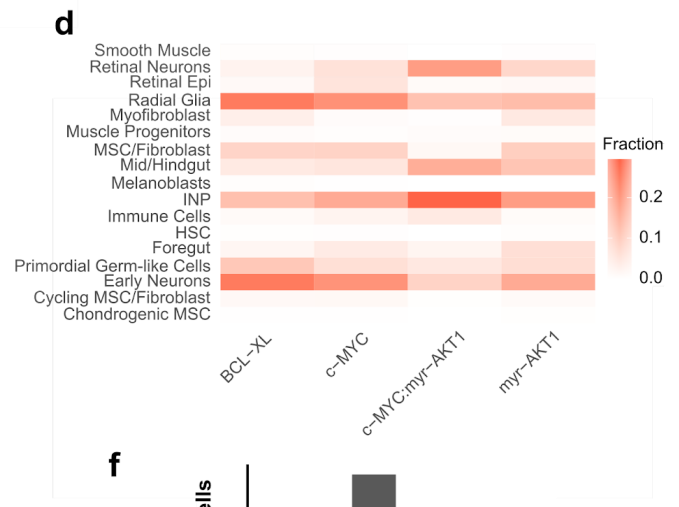
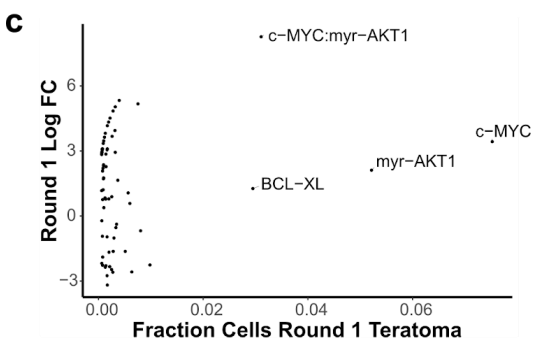
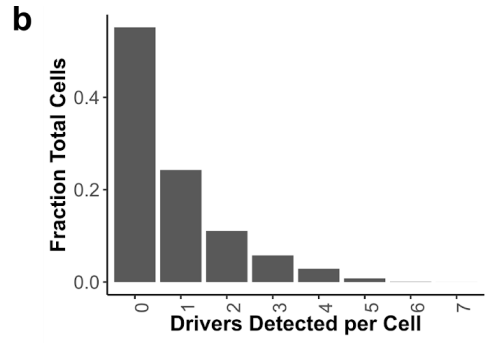
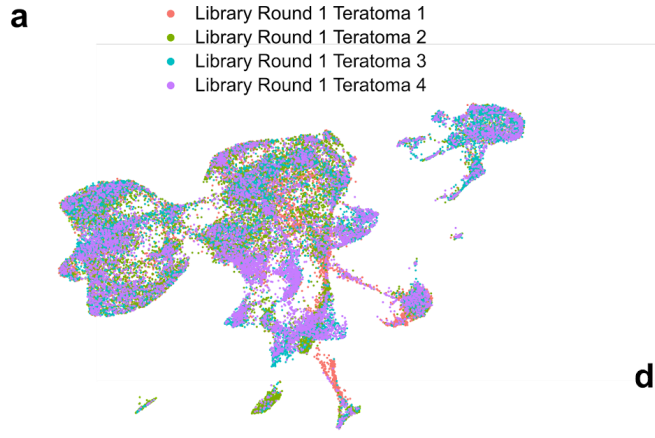
Supplemental information

**Charting oncogenicity of genes and variants across
lineages via multiplexed screens in teratomas**

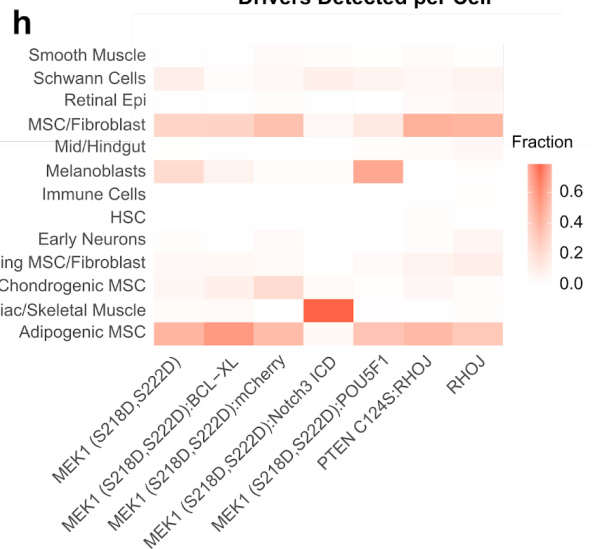
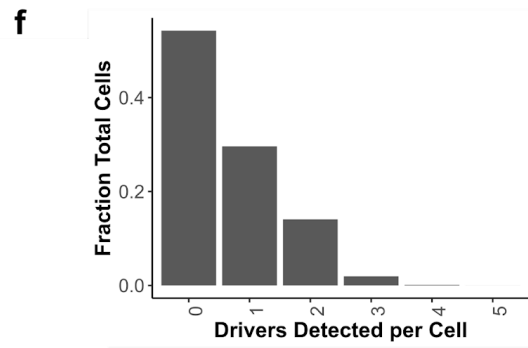
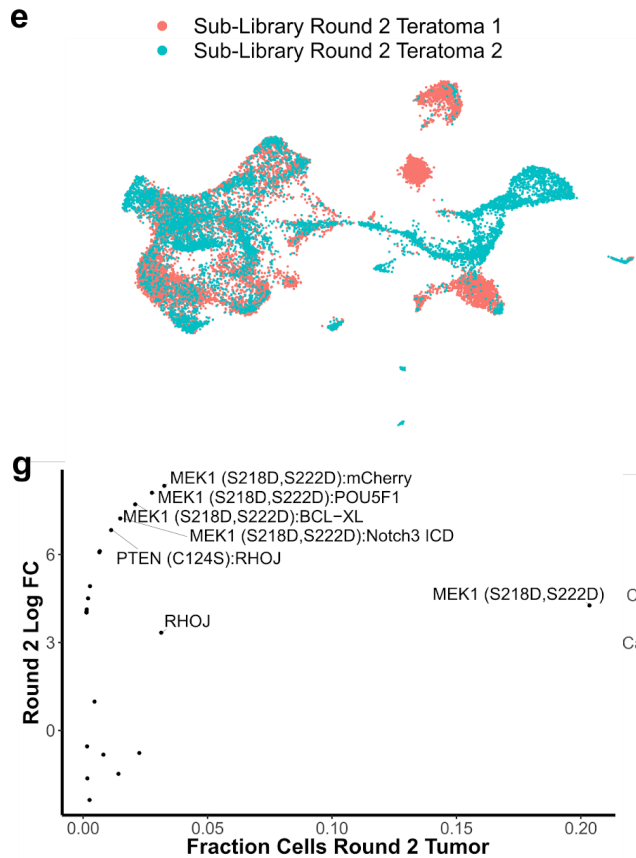
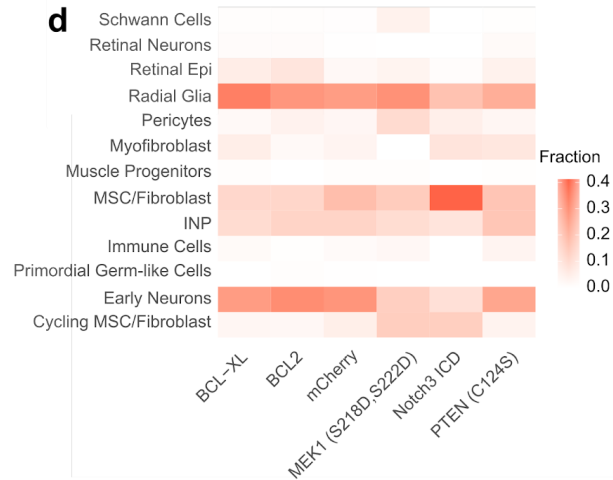
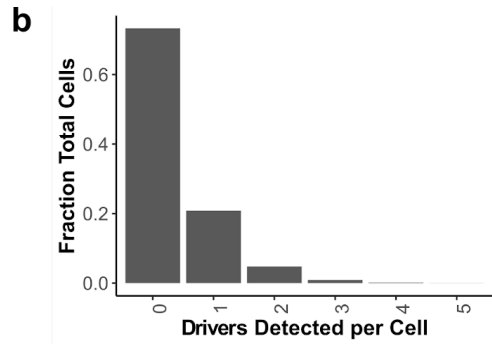
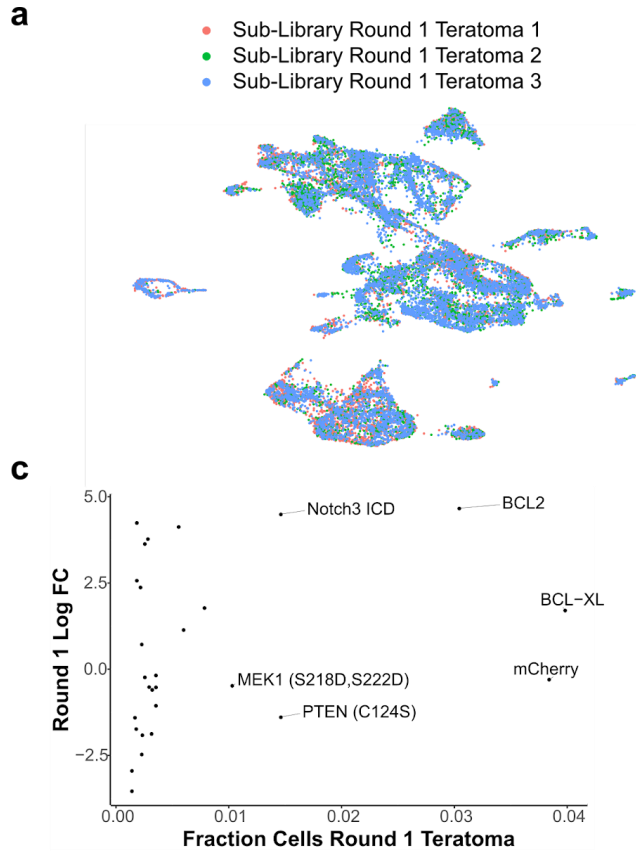
**Udit Parekh, Daniella McDonald, Amir Dailamy, Yan Wu, Thekla Cordes, Kun Zhang, Ann
Tipps, Christian Metallo, and Prashant Mali**

a**b****c****d**

Supplementary Figure 1: Characterization of driver library transduced cells prior to injection, Related to Figure 1. (a) UMAP visualization of cells labelled by cluster identity. (b) Fraction of cells for each number of drivers detected in scRNA-seq for driver library transduced H1 hESCs. (c) Log₂ fold change and significance of proportion of cells in a cluster expressing a driver versus proportion expressing the internal control (mCherry), calculated by permutation testing. Only drivers expressed in 20 or more cells are included. (d) Percentage of reads detecting each library element for barcodes amplified from genomic DNA extracted from driver-library transduced H1 hESCs prior to injection.

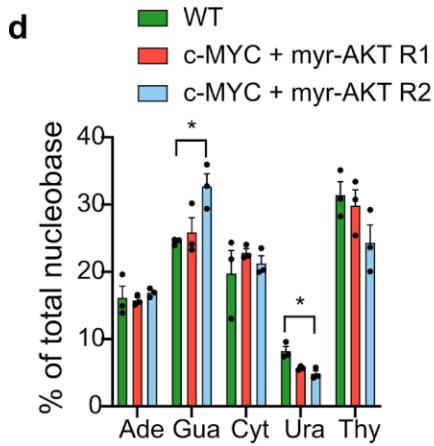
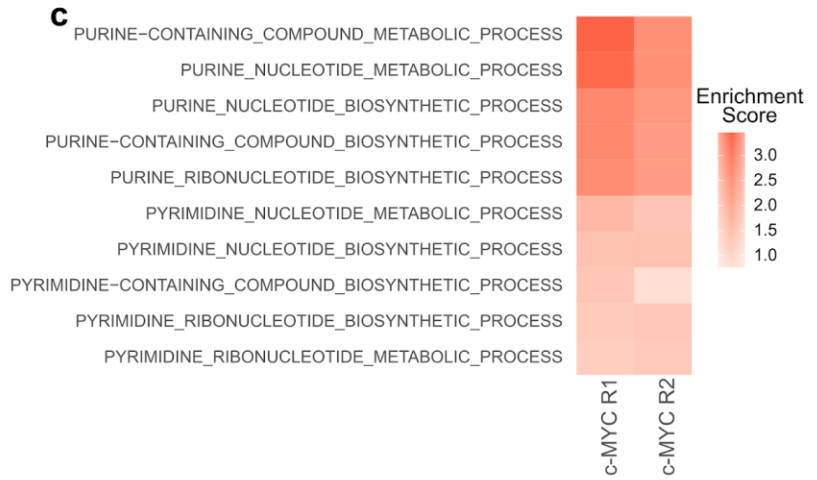
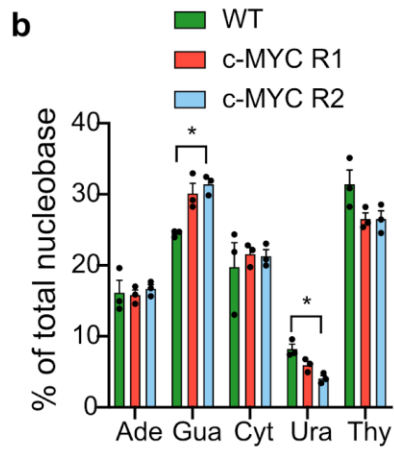
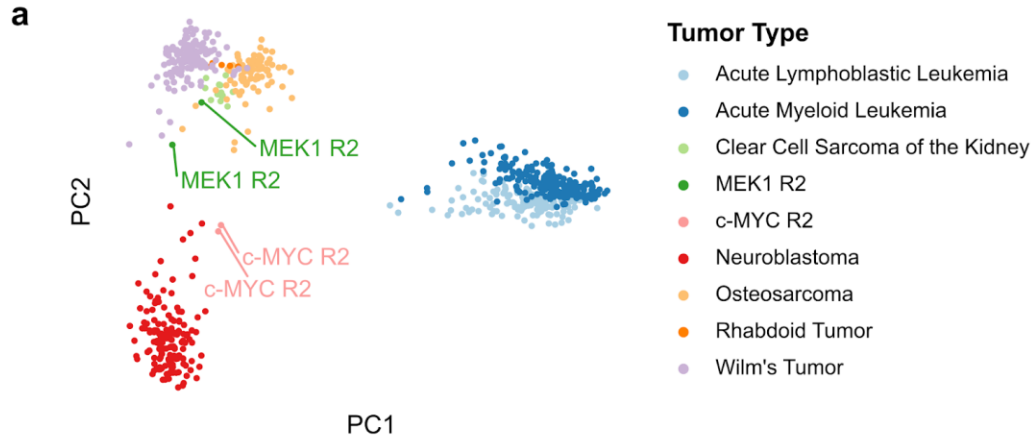


Supplementary Figure 2: Characterization of driver library screen tumors, Related to Figure 2. (a) UMAP visualization of cells by sample from round 1 teratomas formed by driver library transduced hESCs. (b) Fraction of cells for each number of drivers detected in driver library round 1 teratomas. (c) Scatterplot of log fold change of drivers in round 1 teratomas over pre-injection cells, versus fraction of cells in round 1 teratomas for each driver. Only those drivers detected in at least 25 cells across all 4 round 1 teratomas are plotted. Those drivers detected in at least 1% of round 1 teratoma cells are annotated. (d) Heatmap of fraction of cells of each type detected for top detected drivers in round 1 teratomas. (e) UMAP visualization of cells by sample from round 1 teratomas formed by driver library transduced hESCs. (f) Fraction of cells for each number of drivers detected in driver library round 2 tumors. (g) Top enriched hits for each round 2 tumor sample. (h) Scatterplot of log fold change of drivers in round 2 tumors over round 1 teratomas, versus fraction of cells in round 2 tumors for each driver. Only those drivers detected in at least 25 cells across both round 2 tumors are plotted. Those drivers detected in at least 1% of round 2 tumor cells are annotated. (i) Heatmap of fraction of cells of each type detected for top detected drivers in round 2 tumors.



Supplementary Figure 3: Characterization of driver sub-library screen tumors, Related to

Figure 3. (a) UMAP visualization of cells by sample from round 1 teratomas formed by driver sub-library transduced hESCs. (b) Fraction of cells for each number of drivers detected in driver sub-library round 1 teratomas. (c) Scatterplot of log fold change of drivers in round 1 sub-library teratomas over pre-injection cells, versus fraction of cells in round 1 teratomas for each driver. Only those drivers detected in at least 25 cells across all 3 round 1 sub-library teratomas are plotted. Those drivers detected in at least 1% of round 1 teratoma cells are annotated. (d) Heatmap of fraction of cells of each type detected for top detected drivers in round 1 teratomas. (e) UMAP visualization of cells by sample from round 1 teratomas formed by driver sub-library transduced hESCs. (f) Fraction of cells for each number of drivers detected in driver sub-library round 2 tumors. (g) Scatterplot of log fold change of drivers in round 2 tumors over round 1 teratomas, versus fraction of cells in round 2 tumors for each driver. Only those drivers detected in at least 25 cells across both round 2 tumors are plotted. Those drivers detected in at least 1% of round 2 tumor cells are annotated. (h) Heatmap of fraction of cells of each type detected for top detected drivers in round 2 tumors.



Supplementary Figure 4: Metabolic Effects of *c-MYC* and *c-MYC + myr-AKT1*, Related to Figure 4. (a) PC1 vs PC2 plot of *c-MYC* and *MEK1^{S218/S222D}* driven tumors with pediatric tumors from the TARGET initiative. (b) Nucleobase abundance in Control (Wild Type) teratomas, *c-MYC* driven Round 1 tumors and *c-MYC* driven Round 2 tumors. Data represent the mean \pm s.d (* $p \leq 0.05$) (c) Heatmap of enrichment scores for Gene Ontology genesets related to purine and pyrimidine nucleotide metabolism and synthesis for *c-MYC* driven Round 1 and Round 2 tumors compared to wild type teratomas. (d) Nucleobase abundance in Control (Wild Type) teratomas, *c-MYC + myr-AKT1* driven Round 1 tumors and *c-MYC + myr-AKT1* driven Round 2 tumors. Data represent the mean \pm s.d (* $p \leq 0.05$) (e) Heatmap of enrichment scores for Gene Ontology genesets related to purine and pyrimidine nucleotide metabolism and synthesis for *c-MYC + myr-AKT1* driven Round 1 and Round 2 tumors compared to wild type teratomas.